Journal of Vegetation Science 18: 211-220, 2007

Spatial pattern in the organic layer and tree growth: A case study from regenerating *Picea mariana* stands prone to paludification

Lavoie, Martin[1*]; Harper, Karen[2]; Paré, David[3] & Bergeron, Yves[1,4]

[1]*NSERC-UQAT-UQAM Industrial Research Chair in Sustainable Forest Management, Université du Québec en Abitibi-Témiscamingue, 445 Boul. de l'Université, Rouyn-Noranda, QC, J9X 5E4, Canada;* [2]*Department of Biology, Local 3058, Pavillon Alexandre-Vachon, Laval University, Sainte-Foy, QC, G1K 7P4, Canada; karenharper@eastlink.ca;* [3]*Natural Resources Canada, Canadian Forest Service, Laurentian Forestry Center 1055 du PEPS, P.O. Box 10380, Stn. Sainte-Foy, Québec, QC, G1V 4C7, Canada; dpare@exchange.cfl.forestry.ca;* [4]*yves.bergeron@uqat.ca;* [*]*Corresponding author; martin_skifond@hotmail.com*

Abstract

Questions: 1. How does the spatial structure of the organic layer affect tree sapling physiology? 2. Are the organic layer and *Picea mariana* height growth spatially structured at different scales? 3. Does microtopography influence the accumulation of organic matter and does organic layer thickness affect height growth?

Locations: *Picea mariana* forests, northwestern Quebec, Canada.

Methods: We assessed the spatial pattern of each variable in one wildfire site and one harvest site using semivariograms and correlograms. We measured the cross-correlation between relative elevation and organic layer thickness, and between organic layer thickness and growth using cross-correlograms.

Results: *Picea mariana* height growth was autocorrelated to a greater extent in the wildfire site (103 m) than in the harvest site (43 m). The spatial structure of organic layer thickness was similar in both sites. Deeper depressions in the harvest site, as illustrated by spatial variance in relative elevation at short distances (ca. 50 m), and by high autocorrelation values, increased the accumulation of organic matter within 20 m.

Conclusions: The interaction between microtopography and organic matter accumulation led to paludification and poor growth of *Picea mariana* at the harvest site. Paludification at the wildfire site was independent of microtopography and was probably a result of stand development.

Keywords: Forest management; Forested peatland; Geostatistics; Harvest; Microtopography; Productivity; Quebec; Spatial analysis; *Sphagnum*; Wildfire.

Abbreviation: AI = Annual increment.

Introduction

Microtopography and productivity are amongst several factors that can control spatial structure in soil and vegetation (Jenny 1941). Studies in agricultural systems have shown that topography or depth to bedrock can affect the spatial pattern of soil nutrients (Kozar et al. 2002) and plant physiology (Meredieu et al. 1996; Kravchenko & Bullock 2002). The spatial structure of forest stands can also change with stand development (Harper et al. 2005b).

In cold boreal forests, stand development can lead to paludification, an accumulation of organic matter and *Sphagnum* moss cover leading to the formation of waterlogged conditions (Lavoie et al. 2005). By promoting a cold, wet and acidic environment, *Sphagnum* reduces organic matter decomposition rates, microbial activity and nutrient availability (Turetsky 2003; Fenton et al. 2005) resulting in lower tree productivity (Harper et al. 2005a). Paludification can also develop independently of stand development when water and organic matter accumulates in deep hollows in an undulating terrain thereby slowing decomposition. Under these conditions, fire can only reduce the depth of accumulated organic matter slightly (Lavoie et al. 2005).

An analysis of organic layer spatial structure can help distinguish between the two types of paludification. Relative elevation, that is autocorrelated only at short distances and a strong negative correlation between relative elevation and organic layer thickness, would suggest that paludification occurred on undulating terrain. In contrast, weak spatial structure in microtopography and no correlation with organic layer thickness would suggest that paludification occurred during stand development. The ability to differentiate between these two causes of paludification can help managers select the appropriate management strategy to decrease paludification and therefore increase tree productivity.

The overall goal of this study was to investigate the origin of paludification and its effect on *Picea mariana* growth in a six year old harvest site and in a six year old wildfire site. The specific objectives were: (1) to determine the spatial pattern of *Picea mariana* growth, organic layer thickness and relative elevation of the mineral soil (i.e. microtopography) at coarse and fine spatial scales and (2) to assess the relationships between the spatial structures of (a) *Picea mariana* growth and organic layer thickness and (b) organic layer thickness and relative elevation.

Material and Methods

Study area

The study was located in the Lake Matagami Lowland ecological region within the western *Picea mariana*-feathermoss bioclimatic domain (Saucier et al. 1998) in the southwestern James Bay Lowlands physiographic region of Quebec (Fig. 1). This area is typical of the clay belt region in Quebec and Ontario which is characterized by lacustrine deposits left by the glacial lakes Barlow and Ojibway (Vincent & Hardy 1977). The stands were dominated by *Picea mariana* with some *Abies balsamea* and *Larix laricina*. *Rhododendron groenlandicum* dominated the shrub cover with *Kalmia angustifolia* and *Vaccinium* spp., *Sphagnum* moss and feathermosses (mainly *Pleurozium schreberi*) covering the undulating forest floor.

The study area consisted of a wildfire site and a harvest site (Fig. 1) that were considered to be representative of post-disturbed sites of the clay belt on relatively flat terrain with clay deposits. We selected a large (540 km^2) wildfire that burned in 1997; this was the youngest wildfire site available with easy access. Our wildfire site was salvage cut in 1997 and planted with *Picea mariana* in 1998 with no field preparation before planting. A harvest site located close to the wildfire site was of similar age, soil and stand characteristics prior to disturbance. Harvesting was done in 1997 by Cut with Protection of Regeneration and Soils (CPRS but also known as careful logging) with no field preparation or planting after harvesting. Prior to disturbance, forest stands on both sites were more than 175 years old, less than 17 m tall and with less than 60% canopy cover (Anon. 1999a; Bergeron et al. 2004).

Sampling design

Three plots were located in each of the wildfire and harvest sites making a total of six plots (Fig. 1). Plots were at least 500 m apart in the wildfire site and at least 1.5 km apart in the harvest site. Because wildfire is an unplanned natural event, we were restricted to a pseudo-replication design (Hulbert 1984). Such case studies of natural disturbance events can still provide valuable information about disturbance effects but their results must be interpreted cautiously (e.g. Turner et al. 1997; Larson & Franklin 2005). The area covered by each plot varied from 8750 m^2 to 29 000 m^2 and was determined by the size of the cut (for harvest plots), the size of the salvage cut (for wildfire plots) and external limitations (i.e. plots were at least 50 m from any road, forest edge, lake or river). There were four randomly located 40 m × 10 m subplots within each plot making a total of 24 subplots (see Fig. 2 for an example of one plot).

In each subplot, we sampled regenerating trees, relative elevation and organic layer thickness; 30 such trees < 1.3 m were randomly sampled and measured for height and the cumulative growth for the past three

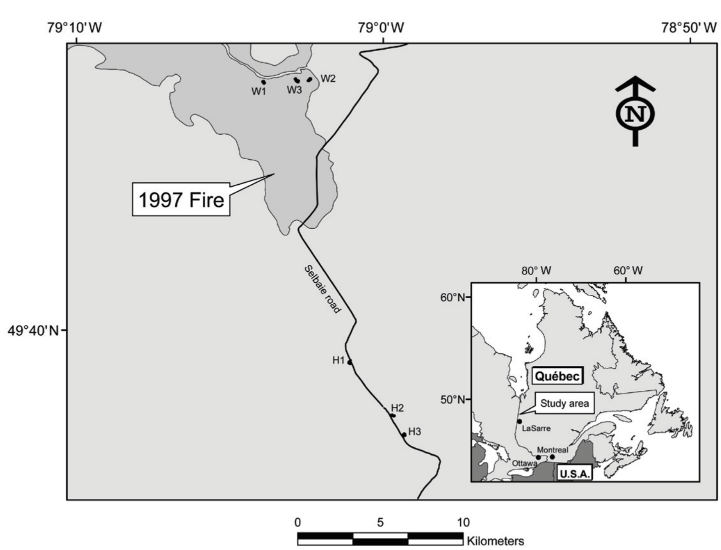

Fig. 1. Location of the study area in Quebec (inset) and locations (circles) of the wildfire (W 1, 2, 3) and harvest (H 1, 2, 3) plots.

years (i.e. 3-year annual increment (AI)). Regenerating trees in the harvest site included seedlings or saplings produced by layering and originated from either before or after the disturbance. In the wildfire site, regenerating trees included only seedlings planted after the fire.

Relative elevation, a measure of the microtopography of the mineral soil, was measured using a sampling grid consisting of 34 points within each subplot (Fig. 2). Relative elevation was defined as the difference in height of the mineral substrate between the sampling point and the height at the base of the theodolite (Theodolite Leica Wild T-2). Measurement at the plot level (i.e. all four subplots combined) was possible only in one wildfire plot and two harvest plots due to long distances between sampling points among subplots. Organic layer thickness was measured with a soil auger next to each tree and at each of the 34 systematic sampling points for a total of 64 samples. Sampling was conducted in 2003.

Statistical analysis

Three year annual increment, organic layer thickness and relative elevation were compared among the six plots using ANOVA. Relationships between three year annual increment and organic layer thickness, as well as between relative elevation and organic layer thickness, were analysed with linear regression analysis. All statistical analyses were computed using SAS 8.02 (Anon. 1999b). Data were checked for normality and equality of variance prior to statistical analyses.

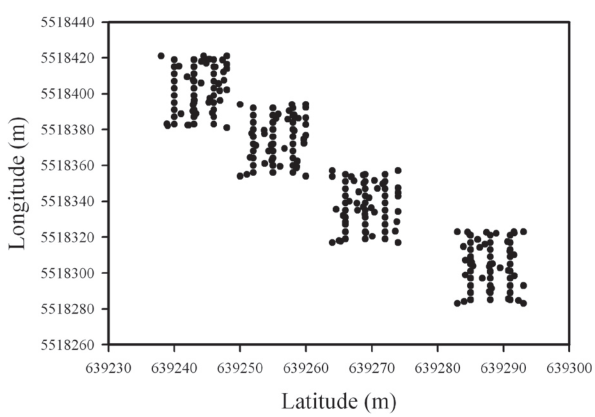

Fig. 2. Sampling design for one plot. Each plot varied in size and included four 10 m × 40 m subplots. Each subplot contained 64 points; 34 of these points were located on a regular sampling grid composed of 30 points at the intersections of three rows (3 m apart) and 10 columns (4 m apart) as well as four additional points at three corners and position [1m 1m]. The remaining 30 points were randomly selected.

Spatial pattern analysis

The spatial structure of three year annual increment, organic layer thickness and relative elevation was examined within each subplot using semivariance and autocorrelation analysis. Each method provides unique information about the spatial pattern. The semivariogram and the correlogram are used in conjunction to evaluate both the range of spatial dependence and the significance of any spatial dependence measured. Moreover, semivariograms measure the portion of the total variance explained by structural variance, while correlograms can determine if autocorrelation is positive or negative. Both tests require the condition of second-order stationarity, meaning that the expected value (mean) and spatial covariance of the variable are the same over the entire study area (Legendre & Legendre 1998). Therefore, all variables were checked for the presence of a broad spatial trend by fitting a first-degree regression equation for each variable as a function of the geographic coordinates. The only variable with a significant geographic trend was relative elevation in wildfire plot 1. In this case, we used the residuals from a trend-surface analysis for subsequent spatial pattern analyses (Legendre & Legendre 1998). For organic layer thickness, spatial analyses were performed for all sampling points combined (n = 64). Semivariograms and correlograms for three year annual increment and organic layer thickness were also performed at the site level (all subplots within each site), and for relative elevation at the plot level (four subplots within each plot).

Semivariograms were used to determine the spatial variance of each variable at different scales using the following estimator (Legendre & Fortin 1989):

$$\gamma(h) = \frac{1}{2N(h)} \sum_{i=1}^{N(h)} [z_1(x_i) - z_1(x_i + h)]^2 \qquad (1)$$

where $\gamma(h)$ is the semivariance at distance interval h; $z(x_i)$ and $z(x_i + h)$ are the values of each variable at locations x_i and $x_i + h$, respectively, and $N(h)$ is number of point-pairs separated by distance h. The results of the semivariogram for each subplot, plot or site were fitted to one of five models: Nugget, Linear, Gaussian, Spherical and Exponential (formulae in App. 1). These fitted models can be classified as exhibiting one of three types of spatial structure. 1. The Nugget model indicated random spatial structure or lack of spatial dependence; the variance is independent of the geographical distance between paired sampling locations. 2. The Linear model, in which the variance increases proportionally with lag distance, indicates that the spatial structure may extend beyond the scale sampled. 3. The remaining models (Gaussian, Spherical, Exponential) exhibit asymptotic spatial structure in which the variance becomes constant after a certain lag distance (Legendre & Fortin 1989). Where possible, various parameters were estimated from the fitted models: (a) the range or the distance at which sample values are no longer correlated (i.e. where a plateau is reached), (b) the sill ($C + C_o$) or the error variance where samples are no longer correlated and c) the nugget (C_o) which is the γ intercept. We calculated structural variance, the proportion of the total model variance [$C / (C + C_o)$], as a measure of spatial dependence (Legendre & Legendre 1998). Structural variance approaches one in a strongly spatially structured system with no nugget semivariance and is close to approach zero (a pure nugget model) in a system with little structure in the range of scale measured. Each semivariogram was calculated with a minimum of 30 data pairs per distance and with a maximum of half the total distance measured in any direction over the sampling space (Rossi et al. 1992). Directionality in the semivariogram analysis was not considered because of the rectangular shape of the sampling area which would have resulted in distances that were too small in one direction (Fortin 1999). Semivariograms were performed using GS+ version 7.0 (Anon. 2005).

For univariate autocorrelation analyses, we used Moran's I coefficient (Moran 1950):

$$I = n \frac{\sum_{ij} w_{ij}\left(y_i - \bar{y}\right)\left(y_j - \bar{y}\right)}{W \sum_{i=1}^{n}\left(y_i - \bar{y}\right)^2} \qquad (2)$$

where y_i is the value of organic layer thickness, three year annual increment, or relative elevation at the i^{th} location, n is the number of points, w_{ij} are the weights in the weight matrix which were allocated with the inverse of the distance between points i and j, and

$$W = \sum_{ij} W_{ij},$$

the sum of the values in the weight matrix. Moran's I is related to Pearson's correlation coefficient and usually ranges between –1 and +1, but can exceed these limits when outliers are present. Positive and negative values of Moran's I indicates that points at a given lag are, generally, more similar or different, respectively, to each other than to the overall mean. Autocorrelations were only computed for distance classes with a minimum of 30 pairs of points (Legendre & Fortin 1989) and only pairs of points separated by less than half the maximum distance observed were considered for the analysis (Rossi et al. 1992). Moran's I coefficient statistics were calculated using the program PASSAGE (Rosenberg 2001). Auto-correlograms were tested for significance following Sokal & Oden (1978). A global test was made by checking whether the correlogram contains at least one value which is significant at the significance level according to the Bonferroni method of correcting for multiple tests (Oden 1984).

Cross-correlations (Rossi et al. 1992) were calculated between three year annual increment and organic layer thickness and between organic layer thickness and relative elevation. A cross-correlogram describes the correlation between two different variables as a function of the distance between samples. When the distance between samples is zero (both variables are sampled at the same location), the cross-correlogram yields the ordinary (non spatial) Pearson correlation coefficient. Cross-correlograms were performed using Variowin 2.2 (Pannetier 1997). For more information on semivariograms, correlograms and cross-correlograms, readers may consult Legendre & Legendre (1998).

We expected that topographic paludification would be evident from (1) a peak in autocorrelation for relative elevation within the scales measured indicating a smaller spatial dependence and (2) negative correlations between *Picea mariana* three year annual increment and organic layer thickness and between organic layer thickness and microtopography. In contrast, if paludification was caused by stand development (prior to the recent disturbance) we expected to find (1) a weak or absent autocorrelation for relative elevation within the scales measured and (2) little or no correlation between regenerating tree growth and organic layer thickness. A lack of influence of organic layer thickness on tree growth would indicate more homogenous environmental conditions created by a relatively flat microtopography of the mineral soil.

Results

Univariate trends

Three-year annual increment and organic layer thickness varied significantly among plots, even within each site (Fig. 3a, b). Three year annual increment was greater in the wildfire plots while the organic layer was thicker in the harvest plots. Microtopography was more variable in harvest plot 2 than in harvest plot 1 or wildfire plot 1 (Fig. 3c).

At a broad scale, structural variance for regenerating tree growth was greater in the harvest site than in the wildfire site (Table 1). However, the spatial range was greater in the wildfire than the harvest site (Fig. 4a, b; Table 1). Correlogram results were similar; regenerating tree growth was positively autocorrelated up to 20 m and 50 m in the harvest and wildfire sites, respectively (Fig. 4c, d). Thus, regenerating trees closer than these distances were more similar in height than trees farther apart.

Spatial structure for organic layer thickness was similar on both sites as shown by a similar range of spatial dependence (Fig. 4e, f; Table 1). However, in the wildfire site, the semivariogram for organic layer thickness shows a hole effect which typically reflects pseudo-periodic or cyclic phenomena. Here, the hole effect relates to the existence of two variance peaks 30 m apart (Fig. 4f). This spatial pattern is also confirmed by the form of the correlogram which shows alternating peaks and troughs (i.e. regions of thick and thin organic layer) ca. 30 m apart (Fig. 4h). In contrast, the form of the correlogram in the harvest site is a single peak suggesting the site contains a single region with a thick organic layer (Fig. 4g). Structural variance for organic layer thickness was slightly higher in the harvest site (Table 1).

For relative elevation in the wildfire plot where analysis was possible, the semivariogram shows a range of spatial dependence of ca. 20 m (Table 1; Fig. 5a) and the form of the correlogram indicates a spatial pattern composed of small peaks and troughs (i.e. high and low relative elevation) separated by 20 m (Fig. 5d). In both harvest plots where analysis was possible, variance peaks in the semivariograms indicate a range of spatial dependence at scales of ca. 40 m (Table 1; Fig. 5b, c). The correlograms show positive autocorrelation in relative elevation up to ca. 20 m for both harvest plots with subsequent negative autocorrelation in plot 2 at greater distances (Fig. 5e, f). However, the form of both correlograms indicate a deep depression in the landscape (i.e. single peak) with a range of influence of ca. 40 m (Fig 5e, f). Structural variance for relative elevation was higher in the harvest site than in the wildfire site (Table 1).

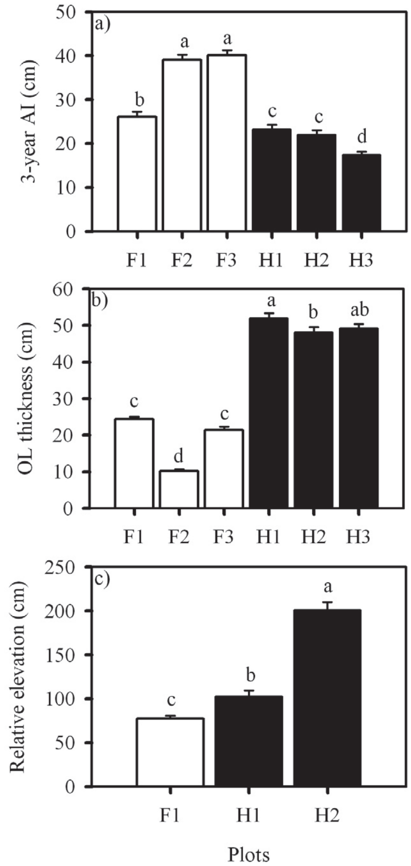

Fig. 3. Means with SE bars in wildfire (F = white bars) and harvest (H = black bars) plots for (**a**) cumulative growth over the past three years (3-year annual increment (AI)) of regenerating *Picea mariana* trees, (**b**) organic layer (OL) thickness and (**c**) relative elevation. Different letters indicate means that are significantly different from one another.

Table 1. Semivariogram model parameters for cumulative growth over the past three years (three year annual increment (AI)) of regenerating *Picea mariana* trees, thickness of the organic layer (OL) and relative elevation in wildfire and harvest sites.

	Plots	Number of sampling points[a]	Sill ($C + C_o$)	Nugget (C_o)	Range (m)	Structural variance $C/(C + C_o)$	Model[b]
Wildfire							
3-year AI	1,2,3	90	5.4	2.4	102.6	0.551	SPH
OL	1,2,3	192	143.2	52.8	33.8	0.631	EXP
Elevation	1	34	262.2	87.4	21.0	0.667	SPH
Harvest							
3-year AI	1,2,3	90	3.66	0.7	43.0	0.809	SPH
OL	1,2,3	192	538.2	165.6	30.3	0.692	SPH
Elevation	1	34	3582.0	10.0	32.2	0.997	GAU
Elevation	2	34	20270.0	0.0	49.4	1.000	GAU

[a] Three-year AI based on 30 points per subplot; elevation based on 34 points per subplot; thickness of the organic layer based on 64 points per subplot.
[b] Model: SPH = Spherical, EXP = Exponential, GAU = Gaussian.

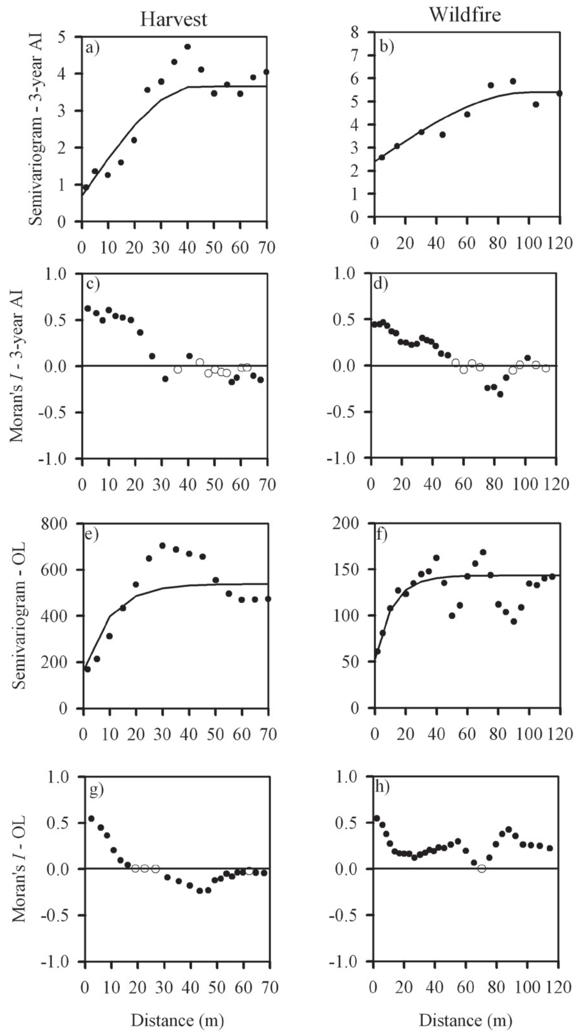

Fig. 4. Auto-semivariograms and auto-correlograms (Moran's *I* coefficient) for (**a**) and (**c**) cumulative growth over the past three years (3 yr annual increment (AI)) of regenerating *Picea mariana* trees in harvest site; (**e**) and (**g**) organic layer (OL) thickness in harvest site; (**b**) and (**d**) cumulative growth over the past three years (3-year annual increment (AI)) of regenerating *Picea mariana* trees in wildfire site; (**f**) and (**h**) organic layer (OL) thickness in wildfire site. The results for the organic layer thickness are based on all 64 sampling points. In the auto-semivariograms, circles represent the semivariance at each distance and black lines represent the fitted semivariogram models. In the auto-correlograms, black circles indicate autocorrelation statistics that were significant after progressive Bonferroni correction (α = 5%) and white circles represent non-significant values.

At the fine scale, regenerating tree growth was randomly distributed (Nugget model) on ca. 60% of the subplots and showed a significant spatial structure (i.e. significant correlogram) on only one third of the subplots (Table 2). For organic layer thickness, the harvest site had more subplots with random spatial distribution as indicated by greater proportions of semivariograms with Nugget models and with correlograms that were not significant, as compared to the wildfire site. Relative elevation had significant spatial structure in most of the subplots, half of which were best fit to linear models which suggests spatial dependence often extended beyond the scales sampled.

Bivariate trends

There was a significant negative linear relationship between organic layer thickness and regenerating tree growth in the wildfire and harvest (Fig. 6a) sites. Although an exponential decay relationship is intuitive, exponential curves were barely indistinguishable from the linear curves in both sites. We expect an exponential relationship, which was about linear over the range of organic layer thickness that we studied. The cross-correlograms indicate that this negative correlation persisted up to distances of ca. 20 m for the harvest site but was generally positive at greater distances (Fig. 7a). In the wildfire, there was no such trend with distance (Fig. 7b).

Overall, relative elevation and organic layer thickness were not significantly related in the wildfire plot (Fig. 6b) but were negatively correlated in harvest plots 1 and 2 (Fig. 6c, d). When regressions were fitted separately, the strength of the relationship between relative elevation and organic layer thickness varied among subplots; correlations were significant in two of the four subplots in the wildfire plot and in three of the four subplots in each of the harvest plots (results not shown). Thus, in the harvest site, organic layer accumulation was reduced on mounds where relative elevation was higher. The cross-correlogram shows that this correlation oscillates between negative and positive at different distances in the wildfire plot (Fig. 7c). In the harvest plots, this correlation switches from negative to positive at lag distances of ca. 20-25 m and remains positive up to 50 m and up to at least 70 m in plots 1 and 2, respectively (Fig. 7d, e).

Discussion

Organic matter accumulated in microtopographic depressions on the harvest site and during stand development on the wildfire site in our study area. However, the origin of the paludification cannot necessarily be

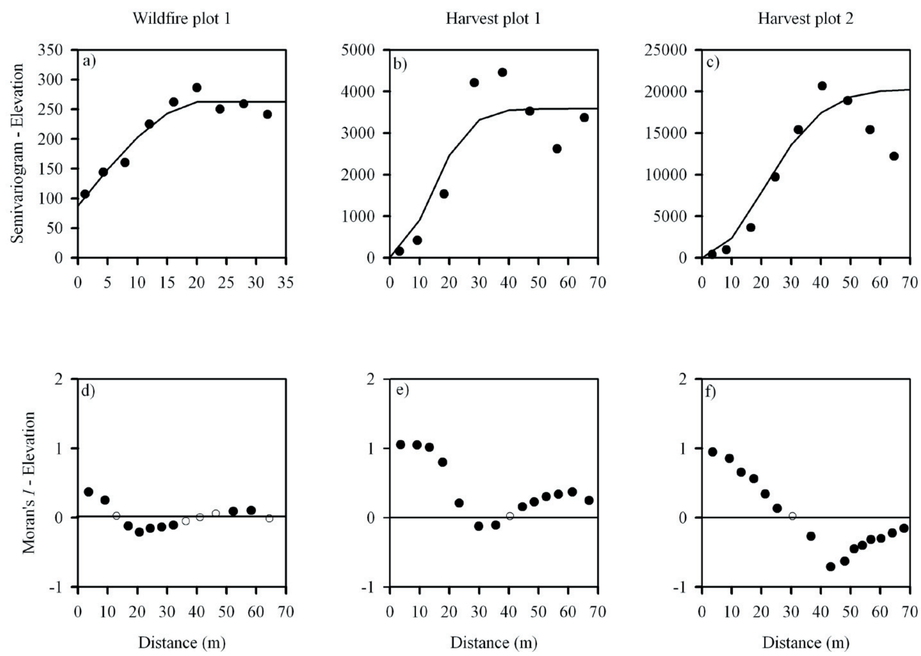

Fig. 5. Spatial statistics for relative elevation in wildfire plot 1 and harvest plots 1 and 2: (**a-c**) auto-semivariograms and (**d-f**) auto-correlograms (Moran's *I* coefficient). In the auto-semivariograms, circles represent the semivariance at each distance and black lines represent the fitted semivariogram models. In the auto-correlograms, black circles indicate autocorrelation statistics that were significant after progressive Bonferroni correction (α = 5%) and white circles represent non-significant values.

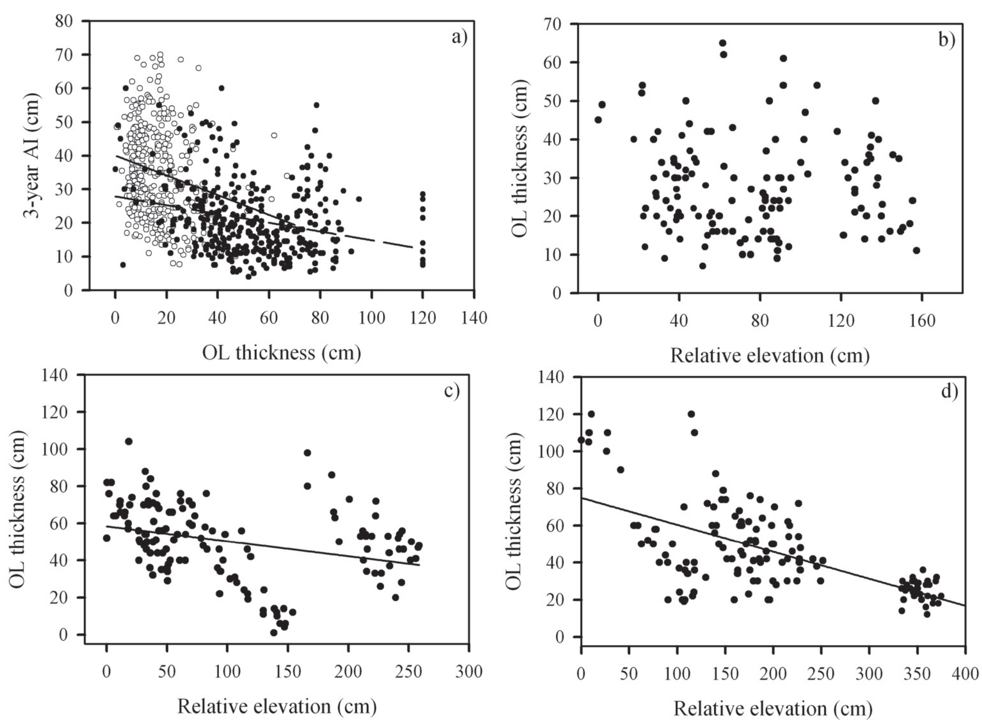

Fig. 6. Non-spatial relationships between variables: cumulative growth over the past three years (3-year annual increment (AI)) of (**a**) regenerating *Picea mariana* trees in relation to organic layer (OL) thickness and (**b**) OL thickness in relation to relative elevation in wildfire plot 1, (**c**) harvest plot 1 and (**d**) harvest plot 2. Regressions (a, c, d) were significant at $P < 0.0001$. In (a), white and black circles represent sampling points in the wildfire and harvest sites, respectively. Lines represent significant linear regressions (R^2 = 0.0530 and 0.0712 for the wildfire (solid line) and harvest (short dash line) sites in a, R^2 = 0.1007 and 0.3849 for c and d, respectively).

Table 2. Number of subplots (max. 12) with nugget, linear and asymptotic models, as well as the number of significant correlograms (Moran's *I*) for cumulative growth over the past three years (3-year annual increment (AI)), thickness of the organic layer (OL) and elevation for wildfire and harvest sites. See App. 2 for detailed results.

	3-year AI [a]	OL thickness [a]	Elevation[a]
Wildfire			
Nugget model	7	2	1
Linear model	0	1	5
Asymptotic model[b]	5	9	6
Moran's *I*	6	9	10
Harvest			
Nugget model	8	6	0
Linear model	0	2	7
Asymptotic model[b]	4	4	5
Moran's *I*	2	7	11

[a] 3-year AI based on 30 points per subplot; elevation based on 34 points per subplot; thickness of the organic layer based on 64 points per subplot.
[b] Asymptotic models include Gaussian, Spherical and Exponential.

attributed to the type of disturbance since the mineral soil layer (which is not affected by disturbance) at the harvest site was more undulating than at the wildfire site. Although the surface topography on the harvest site appeared relatively flat, spatial analysis revealed that the relative elevation of the mineral soil was variable. A negative relationship between relative elevation and organic layer thickness also indicates that organic matter accumulated in hollows of low relative elevation. In contrast, in the wildfire plot where analysis was possible, microtopography was less variable and the relationship between relative elevation and organic layer thickness was weaker. Therefore, it appears as if organic matter accumulated during stand development prior to the fire and was most likely reduced after the fire.

Differences in spatial structure between the harvest and wildfire sites could have been due to the different origin of paludification or disturbance type. Although the extent of autocorrelation of *Picea mariana* growth was greater in the wildfire site than in the harvest site, the spatial pattern of organic layer thickness was similar in both sites. The difference for regenerating tree growth may be due to the different types of regeneration: regularly spaced planted seedlings in the wildfire site vs a more clumped distribution of layers in the harvest site. Although we did not find any evidence several years after planting, the spatial pattern in the wildfire site might also have been affected by the remains of stored nutrients around the planted seedlings. It is possible that even though the soil transported with them was no longer distinguishable from the surrounding soil, nutrients from the transported soil may have affected past growth and created more uniform growth conditions resulting in a more homogenous spatial pattern of tree growth. In Finland, greater homogeneity in stand structure caused by extensive management was also considered an important factor in explaining greater autocorrelation in tree size in managed sites compared to primeval spruce forests

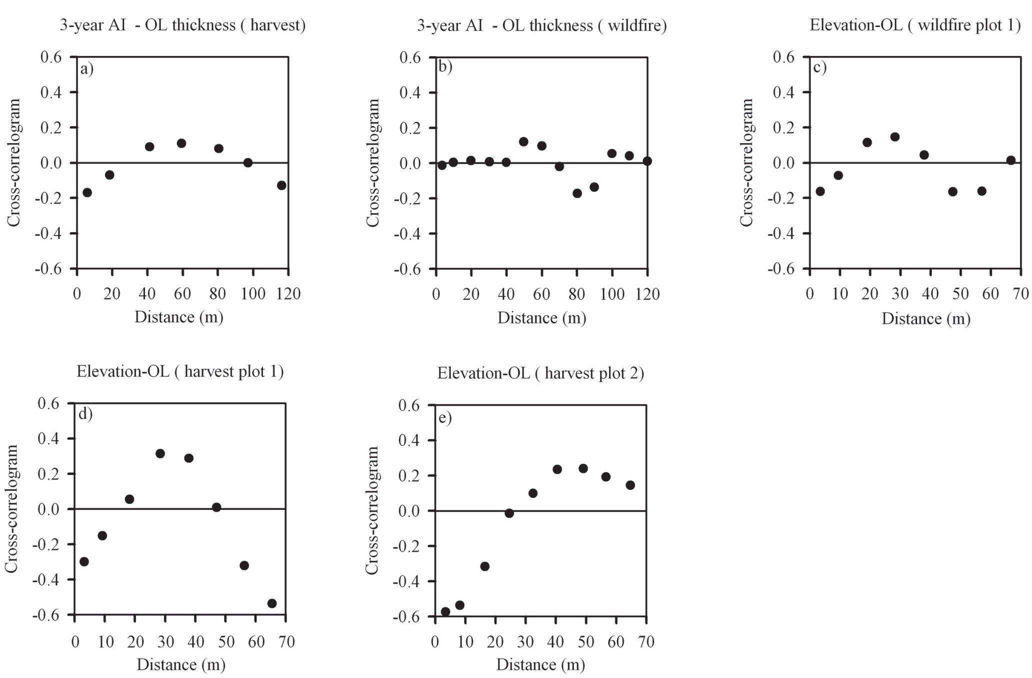

Fig. 7. Cross-correlograms for: cumulative growth over the past three years (3-year annual increment (AI)) of regenerating *Picea mariana* trees and organic layer (OL) thickness in (**a**) the harvest and (**b**) wildfire plots; and for relative elevation and OL thickness in (**c**) wildfire plot 1; (**d**) harvest plot 1 and (**e**) havest plot 2.

(Kuuluvainen et al. 1996).

The variation in the microtopography affected *Picea mariana* growth in the harvest site up to distances of 20-25 m where organic matter accumulation at lower elevations resulted in decreased *Picea mariana* growth. Deep depressions combined with the hard clay soil favoured the accumulation of water and the establishment of *Sphagnum* thereby facilitating the accumulation of low quality organic matter (Lavoie et al. 2005). Poor growth conditions in these deep depressions created a more fine-grained spatial structure of *Picea mariana* growth (Giroux et al. 2001). In contrast, we attribute the near absence of a correlation between regenerating tree growth and organic layer thickness in the wildfire site to more homogenous environmental conditions on a relatively flat layer of mineral soil. The recent wildfire may also have created conditions more favourable to *Picea mariana* growth such as a thinner humus layer, drier soil, higher pH, higher concentration of total and available nutrients and better growth substrates (i.e. material made from feathermosses) as compared to following harvest (Simard et al. 2001; Kasischke & Johnstone, 2005; Lavoie et al. in press). The type of regeneration (planted seedlings vs layers) may also explain greater *Picea mariana* growth in the wildfire site than in the harvest site (Prévost & Dumais 2003).

Forest management strategies differ according to the origin of paludification because of its effect on soil substrate quality. Where paludification develops in depressions of an undulating terrain, the presence of a poorly decomposed organic matter layer combined with wet conditions limits the use of equipment for mechanical site preparation and reduces the success of prescribed burning. In contrast, on sites where paludification occurs during stand development, the accumulated organic matter is well decomposed, creating conditions more appropriate to site preparation. Our method of determining the origin of paludification using spatial pattern analysis could facilitate forest management decisions.

Acknowledgements. We thank Mike Austin and an anonymous reviewer for valuable comments on an earlier version of the manuscript. We thank Benoit Lafleur and Gabriel Diab for technical assistance in the field and Alain Leduc for statistical assistance. The study was funded by the NSERC-UQAT-UQAM Industrial Research Chair in Sustainable Forest Management, the Lake Abitibi Forest Model, Tembec, and the Canadian Forest Service. The senior author received a scholarship from the Natural Science and Engineering Research Council of Canada (NSERC) and from le Fonds Québécois de la Recherche sur la Nature et les Technologies (FQRNT).

References

Anon. 1999a. Carte écoforestière à l'échelle 1/20000. Troisième programme d'inventaire. Direction de la gestion des stocks forestiers. MNRNQ (Ministère des Ressources Naturelles du Québec). Bibliothèque nationale du Québec, Québec, CA.

Anon. 1999b. *The SAS system for Windows Version 8.02*. SAS institute Inc., Cary, NC, US.

Anon. 2005. *Gamma design software*. GS+: *Geostatistics for the environment sciences*. Version 7.0. Plainwell, Michigan, IL, US.

Bergeron, Y., Gauthier, S., Flannigan, M. & Kafka, V. 2004. Fire regimes at the transition between mixedwood and coniferous boreal forest in northwestern Quebec. *Ecology* 85: 1916-1932.

Fenton, N., Lecomte, N., Légaré, S. & Bergeron, Y. 2005. Paludification in black spruce (*Picea mariana*) forests of eastern Canada: Potential factors and management implications. *For. Ecol. Manage*. 213: 151-159.

Fortin, M.-J. 1999. Effects of sampling unit resolution on the estimation of spatial autocorrelation. *Ecoscience* 6: 636-641.

Giroux, J.-F., Bergeron, Y. & Veillette, J.J. 2001. Dynamics and morphology of giant circular patterns of low tree density in black spruce stands in Northern Quebec. *Can. J. Bot.* 79: 420-428.

Harper, K.A., Bergeron, Y., Drapeau, P., Gauthier, S. & De-Granpré, L. 2005a. Structural development following fire in a black spruce boreal forest. *For. Ecol. Manage*. 206: 293-306.

Harper, K.A., Bergeron, Y., Drapeau, P., Gauthier, S. & De-Granpré, L. 2005b. Changes in spatial pattern of trees and snags during structural development in *Picea mariana* boreal forest. *J. Veg. Sci*. 17: 625-636.

Hulbert, S.H. 1984. Pseudoreplication and the design of ecological field experiments. *Ecol. Monogr.* 54: 184-212.

Jenny, H. 1941. *Factors of soil formation*. McGraw-Hill, New York, NY, US.

Kasischke, E.S. & Johnstone, J.F. 2005. Variation in postfire organic layer thickness in a black spruce forest complex in interior Alaska and its effects on soil temperature and moisture. *Can. J. For. Res*. 35: 2164-2177.

Kozar, B., Lawrence, R. & Long, D.S. 2002. Soil phosphorus and potassium mapping using a spatial correlation model incorporating terrain slope gradient. *Prec. Agric*. 3: 407-417.

Kravchenko, A.N. & Bullock, D.G. 2002. Spatial variability of soybean quality as function of field topography: I. Spatial data analysis. *Crop Sci*. 42: 804-815.

Kuuluvainen, T., Penttinen, A., Leinonen, K. & Nygren, M. 1996. Statistical opportunities for comparing structural heterogeneity in managed and primeval forests: An example from boreal spruce forest in southern Finland. *Silva Fenn*. 30: 315-328.

Larson, A.J. & Franklin, J.F. 2005. Patterns of conifer tree regeneration following an autumn wildfire event in the western Oregon Cascade Range, USA. *For. Ecol. Manage*. 218: 25-36.

Lavoie, M., Paré, D., Fenton, N., Groot, A. & Taylor, K.C. 2005. Paludification and management of forested peatlands in Canada: a literature review. *Environ. Rev.* 13: 21-50.

Lavoie, M., Paré, D. & Bergeron, Y. In press. Relationships between micro-site type and the growth and nutrition of young black spruce on post-disturbed lowland black spruce sites. *Can. J. For. Res.*

Legendre, P. & Fortin, M.-J. 1989. Spatial pattern and ecological analysis. *Vegetatio* 80: 107-138.

Legendre, P. & Legendre L. 1998. *Numerical ecology*. 2nd English ed. Elsevier, Amsterdam, NL.

Meredieu, C., Arrouays, D., Goulard, M. & Auclair, D. 1996. Short range soil variability and its effect on red oak growth (*Quercus rubra*). *Soil Sci.* 161: 29-38.

Moran, P.A.P. 1950. Notes on continuous stochastic phenomena. *Biometrika* 37: 17-23.

Oden, N.L. 1984. Assessing the significance of a spatial correlogram. *Geogr. Anal.* 16: 1-16.

Pannetier, Y. 1997. *Variowin software for spatial data analysis in 2D*. Springer Verlag, New York, NY, US.

Prévost, M. & Dumais, D. 2003. Croissance et statut nutritif de marcottes, de semis naturels et de plants d'épinette noire à la suite du scarifiage: résultats de 10 ans. *Can. J. For. Res.* 33 : 2097-2107.

Rosenberg, M.S. 2001. *PASSAGE. Pattern analysis, spatial statistics, and geographic exegesis*. Arizona State University, Tempe, AZ, US.

Rossi, R.E., Mulla, D.J., Journel, A.G. & Franz, E.H. 1992. Geostatistical tools for modelling and interpreting ecological spatial dependence. *Ecol. Monogr.* 62: 277-314.

Saucier, J.P., Bergeron, J.F., Grondin, P. & Robitaille, A. 1998. Les régions écologiques du Québec méridional (3rd version). *L'Aubelle Supplément*, p. 12.

Simard, D.G., Fyles, J.W., Paré, D. & Nguyen, T. 2001. Impacts of clearcut harvesting and wildfire on soil nutrient status in the Quebec boreal forest. *Can. J. Soil Sci.* 81: 229-237.

Sokal, R.R. & Oden, N.L. 1978. Spatial autocorrelation in biology 1. Methodology. *Biol. J. Linn. Soc.* 10: 199-228.

Turetsky, M. 2003. The role of bryophytes in carbon and nitrogen cycling. *Bryologist* 106: 395-409.

Turner, M.G., Romme, W.H., Gardner, R.H. & Hargrove, W.W. 1997. Effects of fire size and pattern on early succession in Yellowstone National Park. *Ecol. Monogr.* 67: 411-433.

Vincent, J.-S. & Hardy, L. 1977. L'évolution et l'extension des lacs glaciaires Barlow et Ojibway en territoire québécois. *Géogr. Phys. Quat.* 31: 357-372.

Received 10 April 2006;
Accepted 4 October 2006;
Co-ordinating Editor: M. Austin.

For App. 1, see also JVS/AVS Electronic Archives; www.opuluspress.se/

App. 1. Formula used to fit the semivariograms to the Spherical, Gaussian, Exponential and Linear models.

Spherical semivariogram model :

$$\gamma_{12}(h) = \begin{cases} 0 & h = 0 \\ C_0 + C\left[\frac{3}{2}\left(\frac{h}{a}\right) - \frac{1}{2}\left(\frac{h}{a}\right)^3\right] & 0 < h < a \\ C_0 + C & h \geq a \end{cases}$$

Gaussian semivariogram model :

$$\gamma_{12}(h) = \begin{cases} 0 & h = 0 \\ C_0 + C\left[1 - \exp(-\left(\frac{3h^2}{a^2}\right)\right] & h > 0 \end{cases}$$

Exponential semivariogram model :

$$\gamma_{12}(h) = \begin{cases} 0 & h = 0 \\ C_0 + C\left[1 - \exp(-\left(\frac{3h}{a}\right)\right] & h > 0 \end{cases}$$

Linear semivariogram model :

$$\gamma_{12}(h) = C_0 + b(C/a)$$

For all these models: (C_o) represents the variance due to sampling error and/or spatial dependence at scales not explicitly sampled; ($C + C_o$) represents the error variance when samples are no longer correlated (i.e., sill); (C) represents the spatially structured component; (a) represents the distance when sample values are no longer correlated (i.e. range); (h) is the effective range; and (b) is the slope.

App. 2. Semivariogram model parameters at the sub-plot (s) level for cumulative growth for the past three years (i.e., 3-year annual increment (AI)), organic layer (OL) thickness and elevation (elev) in wildfire and harvest sites.

				Semivariogram parameters					
	Variable	Grid	Points	Sill($C+C_o$)	Nugget (C_o)	Range (m)	Q $C/(C+C_o)$	Model	R^2
Wildfire									
Plot 1 s 1	AI	R	30	3.3	3.3	-	0.000	NUG	0.054
Plot 1 s 2	AI	R	30	4.3	0.8	27.18	0.826	EXP	0.513
Plot 1 s 3	AI	R	30	3.8	3.8	-	0.000	NUG	0.030
Plot 1 s 4	AI	R	30	2.8	1.1	9.98	0.599	GAU	0.425
Plot 2 s 1	AI	R	30	3.3	3.3	-	0.000	NUG	0.054
Plot 2 s 2	AI	R	30	2.2	2.2	-	0.000	NUG	0.114
Plot 2 s 3	AI	R	30	3.1	3.1	-	0.000	NUG	0.168
Plot 2 s 4	AI	R	30	3.1	0.0	18.5	1.000	GAU	0.557
Plot 3 s 1	AI	R	30	31.4	31.4	-	0.000	NUG	0.000
Plot 3 s 2	AI	R	30	3.8	3.8	-	0.000	NUG	0.126
Plot 3 s 3	AI	R	30	2.6	0.0	17.8	1.000	GAU	0.477
Plot 3 s 4	AI	R	30	3.5	0.0	9.0	1.000	GAU	0.598
Harvest									
Plot 1 s 1	AI	R	30	2.39	0.16	6.1	0.932	SPH	0.179
Plot 1 s 2	AI	R	30	2.1	1.0	15.1	0.500	SPH	0.909
Plot 1 s 3	AI	R	30	1.1	1.1	-	0.000	NUG	0.002
Plot 1 s 4	AI	R	30	0.76	0.38	6.5	0.501	SPH	0.063
Plot 2 s 1	AI	R	30	2.9	2.9	-	0.000	NUG	0.216
Plot 2 s 2	AI	R	30	3.0	3.0	-	0.000	NUG	0.235
Plot 2 s 3	AI	R	30	0.4	0.0	10.0	1.000	EXP	0.006
Plot 2 s 4	AI	R	30	0.9	0.9	-	0.000	NUG	0.320
Plot 3 s 1	AI	R	30	0.3	0.3	-	0.000	NUG	0.028
Plot 3 s 2	AI	R	30	0.1	0.1	-	0.000	NUG	0.061
Plot 3 s 3	AI	R	30	0.8	0.8	0.75	0.000	NUG	0.000
Plot 3 s 4	AI	R	30	0.8	0.8	1.2	0.000	NUG	0.011
Wildfire									
Plot 1 s 1	Elev	S	34	188.4	39.3	31.5	0.788	GAU	0.874
Plot 1 s 2	Elev	S	34	830.9	160.0	31.3	0.807	GAU	0.818
Plot 1 s 3	Elev	S	34	142.6	16.5	12.8	0.885	SPH	NA
Plot 1 s 4	Elev	S	34	205.0	205.0	-	0.000	NUG	0.145
Plot 2 s 1	Elev	S	34	290.0	0.0	25.0	1.000	EXP	0.531
Plot 2 s 2	Elev	S	34	1704.0	93.0	31.5	0.945	EXP	0.953
Plot 2 s 3	Elev	S	34	487.2	26.0	25.7	0.947	GAU	0.913
Plot 2 s 4	Elev	S	34	-	111.0	-	0.000	LIN	NA
Plot 3 s 1	Elev	S	34	-	51.0	-	0.000	LIN	NA
Plot 3 s 2	Elev	S	34	-	10	-	0.000	LIN	NA
Plot 3 s 3	Elev	S	34	-	130.0	-	0.000	LIN	NA
Plot 3 s 4	Elev	S	34	-	80.0	-	0.000	LIN	NA
Harvest									
Plot 1 s 1	Elev	S	34	-	109.0	-	0.000	LIN	NA
Plot 1 s 2	Elev	S	34	813.9	5.0	23.3	0.994	SPH	0.672
Plot 1 s 3	Elev	S	34	920.0	270.0	21.0	0.710	GAU	0.556
Plot 1 s 4	Elev	S	34	499.2	96.0	26.8	0.808	GAU	0.924
Plot 2 s 1	Elev	S	34	-	650.0	-	0.000	LIN	NA
Plot 2 s 2	Elev	S	34	-	420.0	-	0.000	LIN	NA
Plot 2 s 3	Elev	S	34	-	350.0	-	0.000	LIN	NA
Plot 2 s 4	Elev	S	34	878.0	1.0	14.3	0.999	SPH	0.664
Plot 3 s 1	Elev	S	34	-	71.0	-	0.000	LIN	NA
Plot 3 s 2	Elev	S	34	1400.0	0.0	23.0	1.000	SPH	0.870
Plot 3 s 3	Elev	S	34	-	200.0	-	0.000	LIN	NA
Plot 3 s 4	Elev	S	34	-	204.0	-	0.000	LIN	NA
Wildfire									
Plot 1 s 1	OL	S + R	64	86.7	0.0	3.6	1.000	SPH	0.780
Plot 1 s 2	OL	S + R	64	166.5	80.2	35.0	0.518	SPH	0.559
Plot 1 s 3	OL	S + R	64	206.5	35.4	14.4	0.829	EXP	0.691
Plot 1 s 4	OL	S + R	64	-	92.3	-	0.000	LIN	NA
Plot 2 s 1	OL	S + R	64	35.0	0.0	22.0	1.000	EXP	0.023
Plot 2 s 2	OL	S + R	64	25.0	25.0	-	-	NUG	0.129

→

App. 2, cont.

	Variable	Grid	Points	Sill($C+C_o$)	Nugget(C_o)	Range (m)	Q $C/(C+C_o)$	Model	R^2
				Semivariogram parameters					
Plot 2 s 3	OL	S + R	64	104.7	44.2	28.5	0.578	GAU	0.747
Plot 2 s 4	OL	S + R	64	15.0	15.0	-	0.000	NUG	NA
Plot 3 s 1	OL	S + R	64	52.7	26.3	10.0	0.500	SPH	0.574
Plot 3 s 2	OL	S + R	64	447.6	42.2	15.7	0.906	GAU	0.905
Plot 3 s 3	OL	S + R	64	190.0	110.0	30.0	0.395	SPH	0.527
Plot 3 s 4	OL	S + R	64	277.8	77.4	33.0	0.721	GAU	0.734
Harvest									
Plot 1 s 1	OL	S + R	64	187.1	187.1	-	0.000	NUG	0.063
Plot 1 s 2	OL	S + R	64	1100.0	0.0	27.0	1.000	SPH	0.743
Plot 1 s 3	OL	S + R	64	-	16.1	-	0.000	LIN	NA
Plot 1 s 4	OL	S + R	64	173.9	74.5	3.0	0.573	GAU	0.508
Plot 2 s 1	OL	S + R	64	57.1	57.1	-	0.000	NUG	0.016
Plot 2 s 2	OL	S + R	64	-	135.0	-	0.000	LIN	NA
Plot 2 s 3	OL	S + R	64	460.0	164.0	22.4	0.643	GAU	0.784
Plot 2 s 4	OL	S + R	64	240.0	240.0	-	0.000	NUG	0.016
Plot 3 s 1	OL	S + R	64	230.0	230.0	-	0.000	NUG	0.276
Plot 3 s 2	OL	S + R	64	862.0	156.0	14.7	0.819	GAU	0.800
Plot 3 s 3	OL	S + R	64	205.8	205.8	-	0.000	NUG	0.033
Plot 3 s 4	OL	S + R	64	130.3	130.3	-	0.000	NUG	0.002

Note: R = random; S = systematic; Model: SPH = Spherical, EXP = Exponential, LIN = Linear; GAU = Gaussian, NUG = Nugget; Q= structural variance; Sill: $(C+C_o) = C$ indicates the spatially structure variance and C_o represents the variance due to sampling error and/or spatial dependence at scales not explicitly sampled; NA = not available.